

Enhanced hyperthermia performance in hard-soft magnetic mixed $Zn_{0.5}Co_xFe_{2.5-x}O_4/SiO_2$ composite magnetic nanoparticles

Xiang Yu(俞翔), Li-Chen Wang(王利晨), Zheng-Rui Li(李峥睿), Yan Mi(米岩), Di-An Wu(吴迪安), and Shu-Li He(贺淑莉)

Citation: Chin. Phys. B, 2021, 30 (**3**): 036201. DOI: 10.1088/1674-1056/abc67c

Journal homepage: http://cpb.iphy.ac.cn; http://iopscience.iop.org/cpb

What follows is a list of articles you may be interested in

Improvement of high-frequency properties of Co_2FeSi Heusler films by ultrathin Ru underlayer

Cuiling Wang(王翠玲), Shouheng Zhang(张守珩), Shandong Li(李山东), Honglei Du(杜洪磊), Guoxia Zhao(赵国霞), Derang Cao(曹德让)

Chin. Phys. B, 2020, 29 (**4**): 046202. DOI: 10.1088/1674-1056/ab7802

Characterization of CoPt nanowire fabricated by glancing angle deposition

Satoshi Kitai, Zhang Zheng-Jun, Shi Ji, Yoshio Nakamura

Chin. Phys. B, 2015, 24 (**5**): 056201. DOI: 10.1088/1674-1056/24/5/056201

Enhancement of ferromagnetic resonance in Al_2O_3-doped Co_2FeAl Heusler alloy film prepared by oblique sputtering

Li Shan-Dong, Cai Zhi-Yi, Xu Jie, Cao Xiao-Qin, Du Hong-Lei, Xue Qian, Gao Xiao-Yang, Xie Shi-Ming

Chin. Phys. B, 2014, 23 (**10**): 106201. DOI: 10.1088/1674-1056/23/10/106201

Enhancement in solar hydrogen generation efficiency using InGaN photoelectrode after surface roughening treatment with nano-sized Ni mask

Tao Tao, Zhi Ting, Li Ming-Xue, Xie Zi-Li, Zhang Rong, Liu Bin, Li Yi, Zhuang Zhe, Zhang Guo-Gang, Jiang Fu-Long, Chen Peng, Zheng You-Dou

Chin. Phys. B, 2014, 23 (**9**): 096203. DOI: 10.1088/1674-1056/23/9/096203

Controllable synthesis of high aspect ratio $Mg_2B_2O_5$ nanowires and their applications in reinforced polyhydroxyalkanoate composites

Mo Zhao-Jun, Chen Jin-Peng, Lin Jing, Fan Ying, Liang Chun-Yong, Wang Hong-Shui, Xu Xue-Wen, Hu Long, Tang Cheng-Chun

Chin. Phys. B, 2014, 23 (**5**): 056201. DOI: 10.1088/1674-1056/23/5/056201

Enhanced hyperthermia performance in hard-soft magnetic mixed $Zn_{0.5}Co_xFe_{2.5-x}O_4/SiO_2$ composite magnetic nanoparticles*

Xiang Yu(俞翔)†, Li-Chen Wang(王利晨)†, Zheng-Rui Li(李峥睿)†, Yan Mi(米岩), Di-An Wu(吴迪安), and Shu-Li He(贺淑莉)‡

Department of Physics, Capital Normal University, Beijing 100048, *China*

(Received 25 June 2020; revised manuscript received 29 September 2020; accepted manuscript online 31 October 2020)

High quality $Zn_{0.5}Co_xFe_{2.5-x}O_4$ ($x = 0$, 0.05, 0.1, 0.15) serial magnetic nanoparticles with single cubic structures were prepared by the modified thermal decomposition method, and $Zn_{0.5}Co_xFe_{2.5-x}O_4/SiO_2$ composite magnetic nanoparticles were prepared by surface modification of SiO_2. The magnetic anisotropy of the sample increases with the increase of the doping amount of Co^{2+}. When the doping amount is 0.1, the sample shows the transition from superparamagnetism to ferrimagnetism at room temperature. In the $Zn_{0.5}Co_xFe_{2.5-x}O_4/SiO_2$ serial samples, the maximum value of specific loss power (SLP) with 1974 W/g_{metal} can also be found at doping amount of $x = 0.1$. The composite nanoparticles are expected to be an excellent candidate for clinical magnetic hyperthermia.

Keywords: magnetic nanoparticles, magnetic anisotropy, $Zn_{0.5}Co_xFe_{2.5-x}O_4/SiO_2$, magnetic hyperthermia

PACS: 62.23.St, 75.47.Lx, 76.60.Es **DOI:** 10.1088/1674-1056/abc67c

1. Introduction

Iron oxide magnetic nanoparticles (NPs) have wide application prospects in biomedical field, for its advantage of stable chemical properties, excellent biocompatibility, appropriate magnetic properties, simplicity of preparation and tunable nature. The composite nanostructure is made by modifying SiO_2, polyethylene glycol or polydopamine on the surface of the as-obtained NPs. The composite nanostructure displays extremely rich diagnostic and therapeutic functions in the fields of targeted drug release, magnetic resonance imaging, biological magnetic separation and magnetic hyperthermia.[1–8] Magnetic hyperthermia is a new kind of local tumor hyperthermia. Compared with the photo-hyperthermia which mainly uses near infrared laser with lower penetration depth, the alternating current (AC) magnetic field can penetrate into the body tissue to 15 cm and 99% of the electromagnetic energy is not absorbed by the human body.[9] Therefore, magnetic hyperthermia has unique superiorities in the treatment of deep tumors. The hyperthermia performance of traditional Fe_3O_4 magnetic NPs is not very ideal, due to their certain limitations of magnetic properties.[10–12] Therefore, in an actual application process, we have to enhance the dosage of nano materials or the energy of AC field to meet the needs of hyperthermia, which certainly introduces a hidden danger to the safety of magnetic hyperthermia applications.

In order to enhance the magnetic hyperthermia properties of Fe_3O_4-based magnetic NPs, Lee *et al.* prepared magnetic NPs with a core-shell structure ($Zn_{0.4}Co_{0.6}Fe_2O_4@Zn_{0.4}Mn_{0.6}Fe_2O_4$) in 2011. The saturation magnetization and magnetic anisotropy of the samples were effectively adjusted, a maximum specific power loss (SLP) value of 3886 W/g was successfully developed. This can be attributed to the soft and hard magnetic exchange coupling, based on theoretical calculations as a guide. The core-shell NPs can eliminate the tumor tissue of nude mice thoroughly, which is significantly better than the commercial Feridex control group and adriamycin chemotherapy control group.[12] However, because the core-shell NPs need to be grown by seed mediated method repeatedly and the size of the core and shell needs to be precisely controlled, these make the practical application of the samples difficult. In 2018, it was reported that the soft and hard magnetic coupling ferrite NPs were successfully prepared by doping Mn^{2+} and Co^{2+} directly to Fe_3O_4. The preparation of the NPs is easy to achieve, and the SLP value can approach the theoretical limit of 3417 W/g_{metal}. *In vitro* cell hyperthermia experiment, the use of low-dose magnetic NPs can effectively kill tumor cells in a very short time.[13] However, its biocompatibility is significantly lower than Fe_3O_4, which restricts its application *in vivo*. In recent research results, $Zn_{0.5}Fe_{2.5}O_4$ magnetic NPs were reported as typical soft ferrite NPs, which have excellent biocompatibility and good magnetic hyperthermia properties.[14] On the other hand, the theoretical simulation results indicated that the magnetic hyperthermia properties of soft ferrite NPs can be further improved significantly by properly increasing the magnetic anisotropy of the sample.[12]

In this paper, $Zn_{0.5}Co_xFe_{2.5-x}O_4$ ($x = 0$, 0.05, 0.1, 0.15)

*Project supported by the National Natural Science Foundation of China (Grant Nos. 51771124, 51571146, and 51701130).

†These authors contributed equally to this work.

‡Corresponding author. E-mail: shulihe@cnu.edu.cn

© 2021 Chinese Physical Society and IOP Publishing Ltd

serial magnetic NPs were synthesized by doping Zn^{2+} and Co^{2+} ions to Fe_3O_4, to improve the saturation magnetization and magnetic anisotropy of the samples. The SiO_2 shell was modified on the surface of the series of NPs by reverse microemulsion method, to enhance the biocompatibility and water solubility of the NPs. The results show that the magnetic hyperthermia properties of the samples increase first and then decrease with the increase of Co^{2+} doping amount. The peak SLP value of $Zn_{0.5}Co_xFe_{2.5-x}O_4/SiO_2$ samples can reach 1974 W/g_{metal} with $x = 0.1$.

2. Experiments and methods

2.1. Materials

$Fe(acac)_3$, $Zn(acac)_2 \cdot nH_2O$, $Co(acac)_2$ and ammonia (29%) were purchased from Alfa aesar; sodium oleate was purchased from TCI; tetraethyl orthosilicate (TEOS), igepal CO-520 and cyclohexane were purchased from Aldrich; oleic acid and benzyl ether were purchased from Acros.

2.2. Synthesis of $Zn_{0.5}Co_xFe_{2.5-x}O_4$ magnetic nanoparticles

$Zn_{0.5}Co_xFe_{2.5-x}O_4$ magnetic NPs were prepared by the modified thermal decomposition method.[15] Firstly, 2.5 mmol $Fe(acac)_3$, 0.5 mmol $Zn(acac)_2{\cdot}nH_2O$ and $Co(acac)_2$, 2 mmol sodium oleate, 4.5 mL oleic acid and 20 mL benzyl ether were added to the four neck flask. Under the protection of argon, the mixture was heated to 120 °C, and kept for 30 min to remove impurities with low boiling point. Then the mixture was heated to 295 °C with the rate of 10 °C/min, and maintained for 2 h. Finally, the heating device is removed so that the reaction system can be cooled to room temperature, and ethanol is added and centrifuged to separate the NPs.

2.3. Silica coating of $Zn_{0.5}Co_xFe_{2.5-x}O_4$ magnetic nanoparticles

SiO_2 was coated on the surface of NPs via reverse microemulsion method.[16] First, 20 mL cyclohexane and 1.15 mL CO-520 were added to the flask, and mixed thoroughly with sonication bath for 10 min. Then 20 mg $Zn_{0.5}Co_xFe_{2.5-x}O_4$ magnetic NPs and 1 mL cyclohexane were added into an eppendorf tube, thoroughly mixed by sonication bath, and then transferred into the flask. After the mixture was sonicated for 20 min, 0.15 mL ammonia was added dropwise and magnetically stirred for 10 min. Finally, 0.1 mL of TEOS was added and reacted for 24 hours. The as-synthesized $Zn_{0.5}Co_xFe_{2.5-x}O_4/SiO_2$ composite NPs are separated by centrifugation by adding ethanol and hexane.

2.4. Characterization

The morphology of NPs was observed with a transmission electron microscope (TEM, Hitachi H-7650); the high-resolution TEM images were obtained by an FEI Tecnai G2 F30 TEM; the crystal structure was characterized by an x-ray diffractometer (XRD, Bruker D8 advance); the magnetic properties were measured by a commercial superconducting quantum interference device magnetometer (SQUID-VSM). The field-dependent magnetization curves (M–H) were recorded from 0 to ±5 T at 300 K and 10 K. Temperature-dependent magnetization curves (M–T) were measured under zero-field-cooled/field-cooled (ZFC/FC) mode from 10 K to 300 K under a magnetic field of 500 Oe; and the magnetic hyperthermia properties were measured by MSI HYPER 5 machine.

2.5. Calculation of SLP and ILP values

The specific loss power (SLP) is introduced to evaluate the magnetic hyperthermia properties of the samples, which is expressed as

$$\mathrm{SLP} = \frac{CV_\mathrm{s}}{m}\frac{\mathrm{d}T}{\mathrm{d}t}, \tag{1}$$

where C is the volume specific heat capacity, V_s is the volume of the sample, m is the mass of the metallic elements of the NPs in the sample, $\mathrm{d}T/\mathrm{d}t$ is the initial slope of the temperature rise curve.

According to the research, the hyperthermia properties of materials can be more essentially reflected by deducting the amplitude and frequency of AC field from SLP values. Therefore, the intrinsic loss power (ILP) is introduced for evaluation, which is expressed as

$$\mathrm{ILP} = \frac{\mathrm{SLP}}{H^2 f}, \tag{2}$$

where H is the amplitude of the AC field and f is the frequency of the AC field.

2.6. *In vitro* experiments

The cytotoxicity of the $Zn_{0.5}Co_xFe_{2.5-x}O_4/SiO_2$ composite NPs was assessed using *in vitro* cell toxicity assay. Mouse fibroblast cells (MEF) purchased from the American Type Culture Collection were seeded in 96-well plates at a density of 5000 cells per well. Then, different concentrations of the $Zn_{0.5}Co_xFe_{2.5-x}O_4/SiO_2$ composite NPs were added to the wells and incubated for 24 h further. The cell viabilities were determined by the standard Cell Counting Kit-8 (CCK-8, Dojindo, Japan) assay.

3. Results and discussion

Our approach is schematically shown in Fig. 1. $Zn_{0.5}Co_xFe_{2.5-x}O_4$ NPs were synthesized using sodium oleate instead of oleamine and 1,2-hexadecanediol in the classic formulation. This modified thermal decomposition method can save material and time cost more effectively.[15,17–20] Silica coating of $Zn_{0.5}Co_xFe_{2.5-x}O_4$ NPs was performed via the reverse microemulsion method.[16] The hyperthermia properties

of $Zn_{0.5}Co_xFe_{2.5-x}O_4/SiO_2$ composite NPs were systematically studied under AC field.

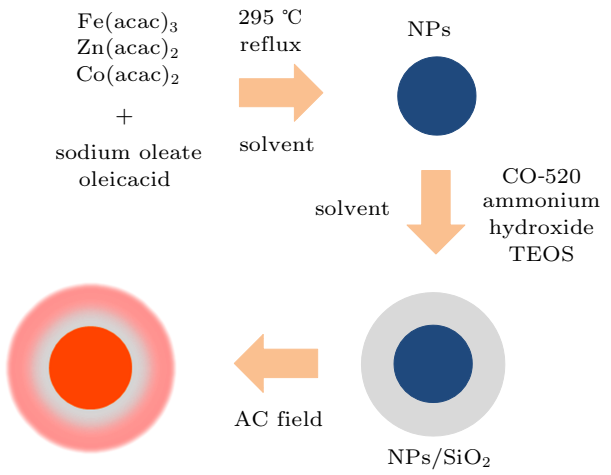


Fig. 1. Scheme of the synthetic route and research method of $Zn_{0.5}Co_xFe_{2.5-x}O_4/SiO_2$ NPs.

As shown in Fig. 2, XRD patterns of $Zn_{0.5}Co_xFe_{2.5-x}O_4$ ($x = 0$, 0.05, 0.1, 0.15) serial NPs and the standard patterns of $Zn_{0.54}Fe_{2.46}O_4$ (PDF card #86-0509, $Fd\bar{3}m$) match so well. All the peaks can be indexed, which indicates that the $Zn_{0.5}Co_xFe_{2.5-x}O_4$ ($x = 0$, 0.05, 0.1, 0.15) serial NPs have single spinel cubic phase structures.

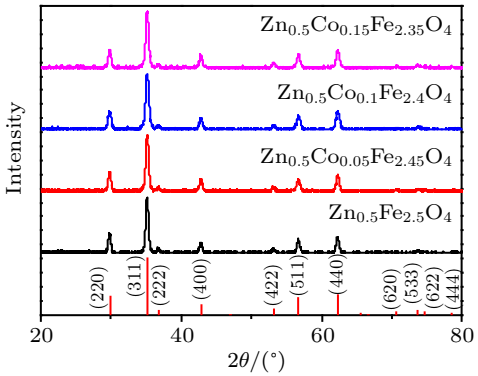


Fig. 2. XRD patterns of $Zn_{0.5}Co_xFe_{2.5-x}O_4$ ($x = 0$, 0.05, 0.1, 0.15) serial NPs.

Using the modified thermal decomposition method, we have synthesized magnetic NPs with controllable size and morphology using sodium oleate instead of oleamine and 1,2-hexadecanediol in the classical formula.[15] It can be seen from Fig. 3 that $Zn_{0.5}Co_xFe_{2.5-x}O_4$ ($x = 0$, 0.05, 0.1, 0.15) serial NPs with stable morphology at 21 nm and good monodispersity were synthesized using the ratio of 3 mmol metal precursor, 2 mmol sodium oleate, 4 mL oleic acid and 20 mL benzyl ether.

The surface of the NPs was coated with SiO_2 via the reverse microemulsion method, as shown in Fig. 4. It can be seen that $Zn_{0.5}Co_xFe_{2.5-x}O_4/SiO_2$ ($x = 0$, 0.05, 0.1, 0.15) serial samples have uniform size, uniform coating of SiO_2 shell, no defect, thickness of about 6 nm, and no formation of free SiO_2 shell. In addition, it can be seen from the high-resolution TEM images that the SiO_2 shell can fully and uniformly coat the magnetic nanoparticle. This can be attribute to the precise control of the volume ratio of ammonia and TEOS in the reaction (0.15 mL : 0.1 mL), in which the concentration of hydrolyzed TEOS monomer is always controlled in the range of heterogeneous nucleation, and the unexpected homogeneous nucleation will be avoided.[16]

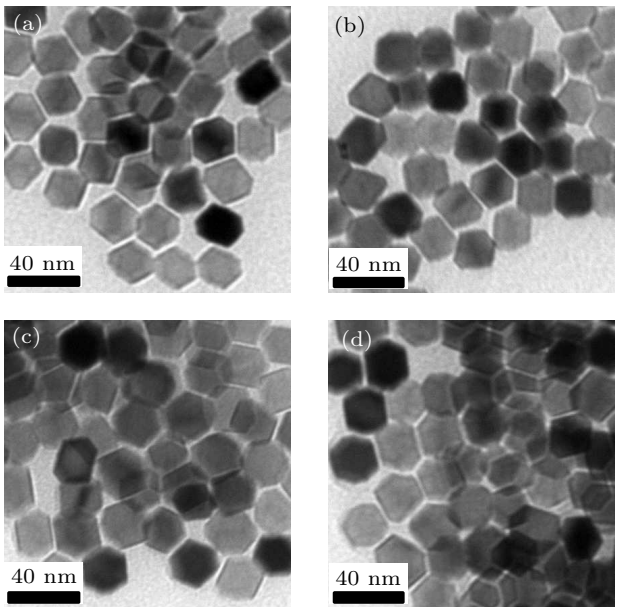


Fig. 3. TEM images of $Zn_{0.5}Co_xFe_{2.5-x}O_4$: (a) $x = 0$, (b) $x = 0.05$, (c) $x = 0.1$, (d) $x = 0.15$ NPs.

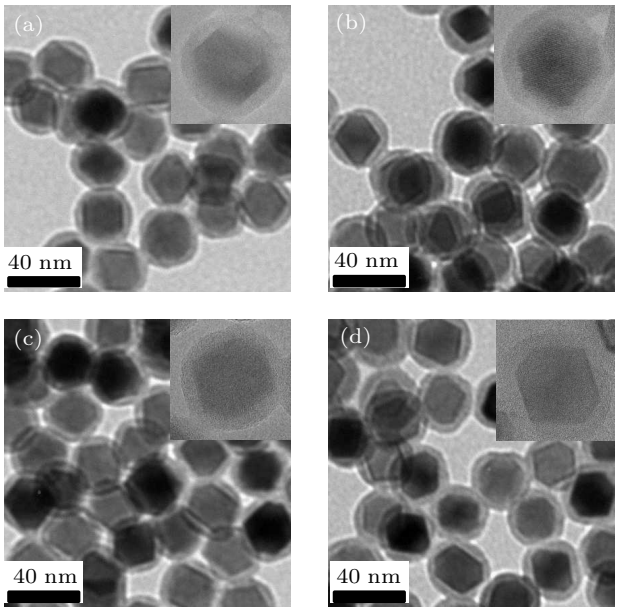


Fig. 4. TEM images of $Zn_{0.5}Co_xFe_{2.5-x}O_4/SiO_2$: (a) $x = 0$, (b) $x = 0.05$, (c) $x = 0.1$, (d) $x = 0.15$ composite NPs. The insets show the high-resolution TEM images of the corresponding $Zn_{0.5}Co_xFe_{2.5-x}O_4/SiO_2$ composite NPs.

The magnetic properties of $Zn_{0.5}Co_xFe_{2.5-x}O_4$ ($x = 0$, 0.05, 0.1, 0.15) serial samples were measured by SQUID-VSM. In earlier research, the saturation magnetization of $Zn_{0.5}Fe_{2.5}O_4$ with Zn^{2+} ion partially replaces Fe^{2+} ions in Fe_3O_4 was effectively enhanced.[21] We further measured the M–H curves of $Zn_{0.5}Co_xFe_{2.5-x}O_4$ serial samples at 300 K and 10 K, as shown in Fig. 5. From the saturation magnetization on the data measured at 300 K, the saturation magnetization decreases monotonously with the increase of the doping amount of Co^{2+} ions. From the doping amount of 0 to 0.15, the saturation magnetization decreases from 85.5 emu/g to 79.3 emu/g. This can be due to the fact that the magnetic moment of original Fe^{2+} ions ($4\mu_B$) is bigger than Co^{2+} ions ($3\mu_B$). In addition, the M–H data measured at 10 K also shows a consistent trend of change, in which the saturation magnetization decreases from 94.2 emu/g to 87.5 emu/g with doping amount from 0 to 0.15. The coercivity (H_c) of the samples increases from 262 Oe to 3500 Oe with the increase of the amount of Co^{2+} ions in the data measured at 10 K, which shows that the doping of traditional hard magnetic Co^{2+} ions can effectively increase the magnetic anisotropy of the samples. The law of coercivity change at 300 K is different from that at 10 K, showing a magnetic phase transition process. The coercivity of the samples remains about 5 Oe with the increase of Co^{2+} ion content from 0 to 0.05, showing a plateau region where the coercivity does not increase with the doping amount. This is normally contributed to superparamagnetism in samples. From the M–T curves shown in Figs. 5(e) and 5(f), it can be seen that the blocking temperature (T_B) of $Zn_{0.5}Fe_{2.5}O_4$ and $Zn_{0.5}Co_{0.05}Fe_{2.45}O_4$ is less than 300 K. Therefore, the results also confirm that the samples have superparamagnetism at room temperature. On the other hand, the coercivity increases to about 11 Oe when the doping amount of Co^{2+} ion is 0.1, and reaches 17 Oe with doping amount of 0.15.

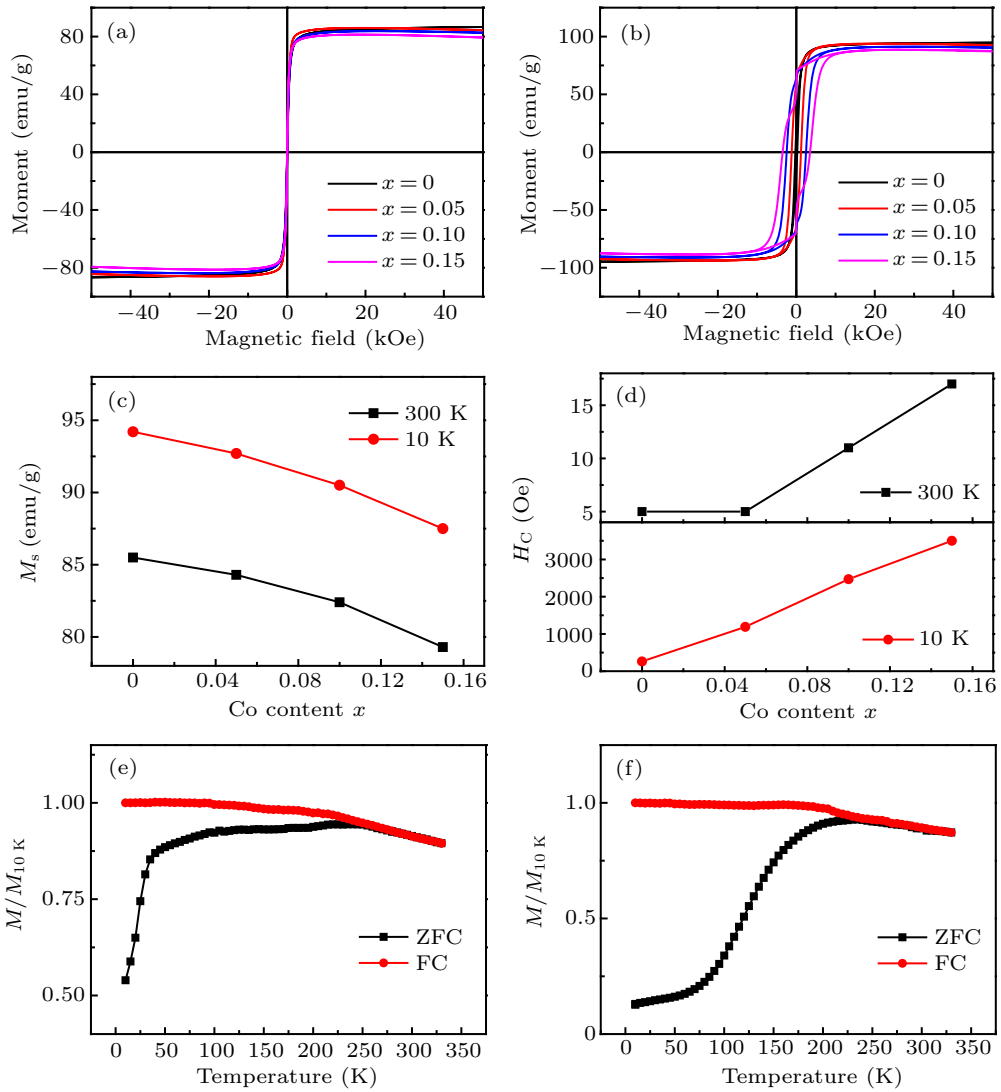


Fig. 5. M–H curves of $Zn_{0.5}Co_xFe_{2.5-x}O_4$ ($x = 0$, 0.05, 0.1, 0.15) NPs at (a) 300 K and (b) 10 K; Co content dependence of (c) saturation magnetization M_s and (d) coercivity H_c for $Zn_{0.5}Co_xFe_{2.5-x}O_4$ NPs, measured at 300 K and 10 K; M–T curves of (e) $Zn_{0.5}Fe_{2.5}O_4$ NPs and (f) $Zn_{0.5}Co_{0.05}Fe_{2.45}O_4$NPs. The curves are normalized to the values at $T = 10$ K.

According to the above phenomenon, the change of the whole magnetic phase can be divided into two sections. It can be inferred that the transition point from superparamagnetism to ferrimagnetism is $x \sim 0.1$ in this study. In addition, we can clearly see from the *M*–*H* curves that there is obvious magnetic phase separation when doping amount is 0.15, which is normally classify as the co-existence of soft and hard magnetic phases. According to the experimental results in the literature, this may be related to the large amount of ion doping in the sample.[15]

The magnetic hyperthermia properties of $Zn_{0.5}Co_xFe_{2.5-x}O_4/SiO_2$ ($x = 0$, 0.05, 0.1, 0.15) serial samples were measured at a concentration of 1 mg/mL, as shown in Fig. 6. The heating performance of the four samples increases monotonously with the increase of AC field amplitude, when the frequency of AC field is maintained at 430 kHz. This is consistent with the description of Rosensweig's theoretical equation[22]

$$P = \mu_0 \pi \chi_0 H^2 f \frac{\omega\tau}{1+(\omega\tau)^2}, \tag{3}$$

where μ_0 is the the vacuum permeability, χ_0 is the equilibrium susceptibility, H is the amplitude of the AC field, f is the frequency of the AC field ($f = \omega/2\pi$), and τ is the total relaxation time of the magnetic NPs in the AC field.

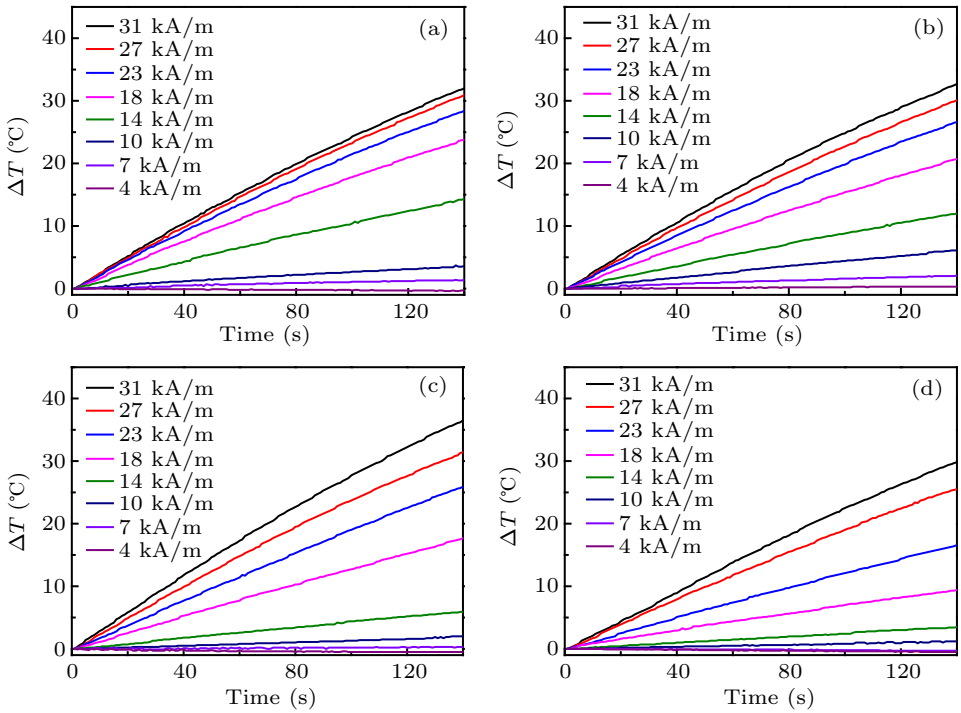


Fig. 6. Heating curves of $Zn_{0.5}Co_xFe_{2.5-x}O_4/SiO_2$ under different magnetic field amplitudes, with the AC field of 430 kHz: (a) $x = 0$, (b) $x = 0.05$, (c) $x = 0.1$, (d) $x = 0.15$.

Using the heating curves of each sample under the highest AC field (31 kA/m, 430 kHz), the corresponding SLP value can be calculated. It can be seen from Fig. 7(a) that the SLP value shows a trend of first increasing and then decreasing with the increase of Co^{2+} ion doping, and reaches the peak value with 1974 W/g_{metal} when $x = 0.1$. It can be concluded that the magnetic hyperthermia properties of $Zn_{0.5}Fe_{2.5}O_4$ samples can be improved by Co^{2+} doping. The earlier literature reported that SLP value does not always monotonously rise, and the best position is near the transition point of magnetic NPs from superparamagnetism to ferrimagnetism.[23–25] In our research, the peak SLP value emerges at $x = 0.1$, consistent with the magnetic measurement data and the explanation in the earlier report.

The magnetic anisotropy continues to increase and the magnetic NPs enter the ferrimagnetic region when the Co^{2+} ions are further increased ($x = 0.15$), which makes the magnetic moment of the sample unable to be effectively reversed by the AC field. On the other hand, the saturation magnetization of the sample has dropped to 79.3 emu/g when the doping amount is $x = 0.15$. According to the research results of the literature, the loss power will also be significantly reduced.[12] Finally, it can be seen from the change diagram of SLP value with Co^{2+} doping amount that the SLP value will be significantly decreased at this time.

On the other hand, the total relaxation time, which is composed of Brown relaxation time and Néel relaxation time, will affect the loss power, from the formula of linear response theory. In this paper, the Néel relaxation time will be mainly affected by adjusting the magnetic anisotropy of the sample,

which is expressed as

$$\tau_N = \tau_0 \exp \frac{KV}{k_B T}, \tag{4}$$

where τ_0 is the time constant ($\tau_0 \sim 10^{-9}$ s), K is the anisotropy constant, V is the volume of nanoparticle, and k_B is the Boltzmann constant. In the literature, a theoretical simulation is made based on the linear response theory. From the simulation results, it can be clearly seen that there is a non-monotonic response relationship between the anisotropy constant K and the SLP value of the magnetic NPs. That is, with the increase of the anisotropy constant, the SLP value presents a process of increasing first and then decreasing. This means that under a certain AC field, magnetic NPs need to have an appropriate K value to obtain the maximum SLP value. In our work, the variation of SLP with the anisotropic constant K is in good agreement with the theoretical simulation in the literature. An optimal K value under the AC field is achieved when the Co^{2+} ion doping amount is 0.1. Therefore, it has the highest SLP value in the series of samples.[12,22,26,27]

The change chart of ILP with the amount of Co^{2+} ion doping is obtained by removing the influence of AC field amplitude and frequency from the SLP value. As shown in Fig. 7(b), it can be seen from the chart that the trend of ILP values is consistent with the change of SLP values with the amount of Co^{2+} ion doping, with a peak value of 4.77 nHm^2/kg_{metal} with Co^{2+} ion doping amount is 0.1.

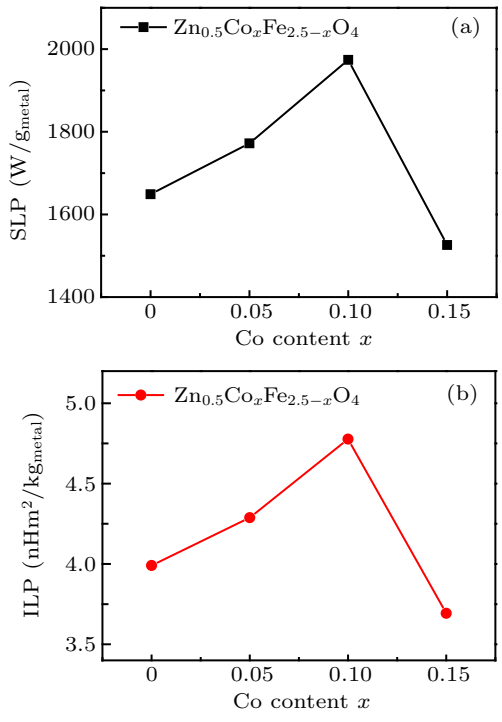


Fig. 7. (a) SLP and (b) ILP for $Zn_{0.5}Co_xFe_{2.5-x}O_4/SiO_2$ composite NPs under the AC field of 430 kHz and 31 kA/m.

Cytotoxicity of $Zn_{0.5}Co_xFe_{2.5-x}O_4/SiO_2$ composite NPs to MEF cells was measured and studied. The different concentrations of $Zn_{0.5}Co_xFe_{2.5-x}O_4/SiO_2$ composite NPs ranging from 25 to 1000 μg/mL were incubated with the cells for 24 h. After the incubation period, the viability of the MEF cells was assessed by CCK-8. Cells without NPs were used as control groups. Compared to the group without NPs, as shown in Fig. 8, the group containing different concentrations of $Zn_{0.5}Co_xFe_{2.5-x}O_4/SiO_2$ composite NPs shows no significant difference in cell viability at the incubation time of up to 24 h. Though at 1000 μg/mL after incubation for 24 h, viability of MEF cells with NPs is nearly 100%, which suggests that the materials are biocompatible.

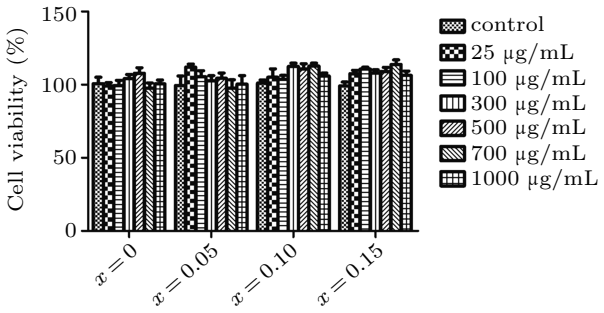


Fig. 8. The viability of the MEF cells determined by CCK-8 assay after incubation in NP solutions with various concentrations for 24 h.

4. Conclusion

In summary, a series of high-quality $Zn_{0.5}Co_xFe_{2.5-x}O_4$ (x = 0, 0.05, 0.1, 0.15) samples were synthesized by the modified thermal decomposition method. The saturation magnetization of the sample is improved and the magnetic anisotropy of the sample is controlled by doping Zn^{2+} and Co^{2+} ions into Fe_3O_4. A transition point from superparamagnetism to ferrimagnetism is found with Co^{2+} content of 0.1. A peak SLP value of 1974 W/g_{metal} has been found in $Zn_{0.5}Co_{0.1}Fe_{2.4}O_4/SiO_2$, which corresponds to the magnetic properties. In addition, the NPs show excellent biocompatibility *in vitro*. The composite NPs are expected to be a good candidate material in applications of magnetic hyperthermia.

References

[1] Liu X, Zheng J, Sun W, Zhao X, Li Y, Gong N, Wang Y, Ma X, Zhang T, Zhao L, Hou Y, Wu Z, Du Y, Fan H, Tian J and Liang X 2019 *ACS Nano* **13** 8811

[2] Guisasola E, Asín L, Beola L, de la Fuente J M, Baeza A and Vallet-Regí M 2018 *ACS Appl. Mater. Interfaces* **10** 12518

[3] Tay Z W, Chandrasekharan P, Chiu-Lam A, Hensley D W, Dhavalikar R, Zhou X Y, Yu E Y, Goodwill P W, Zheng B, Rinaldi C and Conolly S M 2018 *ACS Nano* **12** 3699

[4] Wang B, Chan K F, Yu J, Wang Q, Yang L, Chiu P W Y and Zhang L 2018 *Adv. Funct. Mater.* **28** 1705701

[5] Guo Y, Zhang Y, Ma J, Li Q, Li Y, Zhou X, Zhao D, Song H, Chen Q and Zhu X 2018 *J. Control. Release* **272** 145

[6] Albarqi H A, Wong L H, Schumann C, Sabei F Y, Korzun T, Li X, Hansen M N, Dhagat P, Moses A S, Taratula O and Taratula O 2019 *ACS Nano* **13** 6383

[7] Wu H, Liu L, Song L, Ma M, Gu N and Zhang Y 2019 *ACS Nano* **13** 14013

[8] Zhao L Y, Liu J Y, Ouyang W W, Li D Y, Li L, Li L Y and Tang J T 2013 *Chin. Phys. B* **22** 108104
[9] Derfus A M, von Maltzahn G, Harris T J, Duza T, Vecchio K S, Ruoslahti E and Bhatia S N 2007 *Adv. Mater.* **19** 3932
[10] Chen R, Christiansen M G, Sourakov A, Mohr A, Matsumoto Y, Okada S, Jasanoff A and Anikeeva P 2016 *Nano Lett.* **16** 1345
[11] Dutz S, Clement J H, Eberbeck D, Gelbrich T, Hergt R, Müller R, Wotschadlo J and Zeisberger M 2009 *J. Magn. Magn. Mater.* **321** 1501
[12] Lee J H, Jang J T, Choi J, Moon S H, Noh S H, Kim J W, Kim J G, Kim I S, Park K I and Cheon J 2011 *Nat. Nanotechnol.* **6** 418
[13] He S, Zhang H, Liu Y, Sun F, Yu X, Li X, Zhang L, Wang L, Mao K, Wang G, Lin Y, Han Z, Sabirianov R and Zeng H 2018 *Small* **14** 1800135
[14] Wang R, Liu J, Liu Y, Zhong R, Yu X, Liu Q, Zhang L, Lv C, Mao K and Tang P 2020 *R. Soc. Open Sci.* **7** 191139
[15] Wu L, Jubert P, Berman D, Imaino W I, Nelson A, Zhu H, Zhang S and Sun S 2014 *Nano Lett.* **14** 3395
[16] Ding H L, Zhang Y X, Wang S, Xu J M, Xu S C and Li G H 2012 *Chem. Mater.* **24** 4572
[17] Sun S, Zeng H, Robinson D B, Raoux S, Rice P M, Wang S X and Li G 2004 *J. Am. Chem. Soc.* **126** 273
[18] Webers S, Hess M, Landers J, Schmidt A M and Wende H 2020 *ACS Appl. Polym. Mater.* **2** 2676
[19] Lavorato G C, Das R, Xing Y, Robles J, Litterst F J, Baggio-Saitovitch E, Phan M H and Srikanth H 2020 *ACS Appl. Nano Mater.* **3** 1755
[20] Muro-Cruces J, Roca A G, López-Ortega A, Fantechi E, del-Pozo-Bueno D, Estradé S, Peiró F, Sepúlveda B, Pineider F, Sangregorio C and Nogues J 2019 *ACS Nano* **13** 7716
[21] Guillaud C 1951 *J. Phys. Rad.* **12** 239
[22] Rosensweig R E 2002 *J. Magn. Magn. Mater.* **252** 370
[23] Wu L, Mendoza-Garcia A, Li Q and Sun S 2016 *Chem. Rev.* **116** 10473
[24] Mehdaoui B, Meffre A, Carrey J, Lachaize S, Lacroix L M, Gougeon M, Chaudret B and Respaud M 2011 *Adv. Funct. Mater.* **21** 4573
[25] Hergt R, Hiergeist R, Zeisberger M, Glöckl G, Weitschies W, Ramirez L P, Hilger I and Kaiser A W 2004 *J. Magn. Magn. Mater.* **280** 358
[26] Wang X, Gu H and Yang Z 2005 *J. Magn. Magn. Mater.* **293** 334
[27] Dutz S and Hergt R 2013 *Int. J. Hyperthermia* **29** 790